JCI The Journal of Clinical Investigation

Activated endothelial cells elicit paracrine induction of epithelial chloride secretion. 6-Keto-PGF1alpha is an epithelial secretagogue.

E D Blume, … , G L Stahl, S P Colgan

J Clin Invest. 1998;102(6):1161-1172. https://doi.org/10.1172/JCI3465.

Research Article

Endothelial cells play a central role in the coordination of the inflammatory response. In mucosal tissue, such as the lung and intestine, endothelia are anatomically positioned in close proximity to epithelia, providing the potential for cell-cell crosstalk. Thus, in this study endothelial-epithelial biochemical crosstalk pathways were studied using a human intestinal crypt cell line (T84) grown in noncontact coculture with human umbilical vein endothelia. Exposure of such cocultures to endothelial-specific agonists (LPS) resulted in activation of epithelial electrogenic Cl- secretion and vectorial fluid transport. Subsequent experiments revealed that in response to diverse stimuli (LPS, IL-1alpha, TNF-alpha, hypoxia), endothelia produce and secrete a small, stable epithelial secretagogue into conditioned media supernatants. Further experiments identified this secretagogue as 6-keto-PGF1alpha, a stable hydrolysis product of prostacyclin (PGI2). Results obtained with synthetic prostanoids indicated that 6-keto-PGF1alpha (EC50 = 80 nM) and PGI2 stable analogues (EC50 = 280 nM) activate the same basolaterally polarized, Ca2+-coupled epithelial receptor. In summary, these findings reveal a previously unappreciated 6-keto-PGF1alpha receptor on intestinal epithelia, the ligation of which results in activation of electrogenic Cl- secretion. In addition, these data reveal a novel action for the prostacyclin hydrolysis product 6-keto-PGF1alpha and provide a potential endothelial- epithelial crosstalk pathway in mucosal tissue.

Activated Endothelial Cells Elicit Paracrine Induction of Epithelial Chloride Secretion

6-keto-$PGF_{1\alpha}$ Is an Epithelial Secretagogue

Elizabeth D. Blume, Cormac T. Taylor, Paul F. Lennon, Gregory L. Stahl, and Sean P. Colgan
Center for Experimental Therapeutics and Reperfusion Injury, Department of Anesthesia, Brigham and Women's Hospital, and Department of Cardiology, Children's Hospital and Harvard Medical School, Boston, Massachusetts 02115

Abstract

Endothelial cells play a central role in the coordination of the inflammatory response. In mucosal tissue, such as the lung and intestine, endothelia are anatomically positioned in close proximity to epithelia, providing the potential for cell–cell crosstalk. Thus, in this study endothelial–epithelial biochemical crosstalk pathways were studied using a human intestinal crypt cell line (T84) grown in noncontact coculture with human umbilical vein endothelia. Exposure of such cocultures to endothelial-specific agonists (LPS) resulted in activation of epithelial electrogenic Cl^- secretion and vectorial fluid transport. Subsequent experiments revealed that in response to diverse stimuli (LPS, IL-1α, TNF-α, hypoxia), endothelia produce and secrete a small, stable epithelial secretagogue into conditioned media supernatants. Further experiments identified this secretagogue as 6-keto-$PGF_{1\alpha}$, a stable hydrolysis product of prostacyclin (PGI_2). Results obtained with synthetic prostanoids indicated that 6-keto-$PGF_{1\alpha}$ (EC_{50} = 80 nM) and PGI_2 stable analogues (EC_{50} = 280 nM) activate the same basolaterally polarized, Ca^{2+}-coupled epithelial receptor. In summary, these findings reveal a previously unappreciated 6-keto-$PGF_{1\alpha}$ receptor on intestinal epithelia, the ligation of which results in activation of electrogenic Cl^- secretion. In addition, these data reveal a novel action for the prostacyclin hydrolysis product 6-keto-$PGF_{1\alpha}$ and provide a potential endothelial–epithelial crosstalk pathway in mucosal tissue. (*J. Clin. Invest.* 1998. 102:1161–1172.) Key words: inflammation • intestine • ion transport • prostaglandin • sepsis

Introduction

Mucosal epithelial cells provide a barrier that separates lumenal and vascular compartments. This monolayer of cells provides barrier function and serves as a conduit for vectorial ion movement, the transport event responsible for mucosal hydration and, in excess, secretory diarrhea (1). By secreting solutes and transporting fluid across the epithelium, epithelia are able to coordinate compositional changes of the lumenal compartment. Several stimuli, including hormones, neurotransmitters, and cytokines have been shown to directly regulate both epithelial barrier function and ion transport (1–3).

In intact mucosal tissues, including the lung and intestine, epithelial cells are anatomically positioned in close proximity to a number of subepithelial cell types, including lymphocytes, fibroblasts, smooth muscle cells, and endothelia. These subepithelial cell populations contribute to epithelial function through paracrine pathways. For instance, PG synthesis in the intestine is derived almost exclusively from subepithelial populations (4). The vascular endothelium functions as more than a passive conduit for blood components, and synthesizes many compounds which precisely regulate blood vessel tone, vascular composition, and leukocyte movement (5–7). Endothelial cells themselves respond to a variety of proinflammatory stimuli, including TNF-α, IL-1, and endotoxin and in turn release inflammatory mediators such as cytokines and bioactive lipids (6). The vital role of the endothelium in coordinating inflammation and the proximity of the vasculature to the epithelium provide a potential paracrine crosstalk pathway between these two cell types.

Based on these previous studies, we developed a system to ask focused questions regarding endothelial–epithelial crosstalk in vitro. A noncontact, coculture system was used to examine endothelial paracrine compounds which influence epithelial functional responses. Our results revealed that endothelial-specific agonists activate the production and release of an endothelial secretagogue (termed endothelial-derived secretagogue, EDS)[1] which binds a basolaterally polarized epithelial receptor and induces epithelial Cl^- secretion and fluid transport. The present studies identified EDS as 6-keto-$PGF_{1\alpha}$ and defined a basolaterally polarized, Ca^{2+}-coupled 6-keto-$PGF_{1\alpha}$ receptor, the ligation of which induces electrogenic Cl^- secretion.

Methods

Materials

Where indicated, endothelial monolayers were exposed to LPS from *Escherichia coli* (List Biological Laboratories, Inc., Cambell, CA), recombinant human IL-1α or TNF-α (both from R&D Systems, Minneapolis, MN), indomethacin (Sigma Chemical Co., St. Louis, MO), or

Address correspondence to Sean P. Colgan, Ph.D., Center for Experimental Therapeutics and Reperfusion Injury, Brigham and Women's Hospital, Thorn Bldg. 704, 75 Francis Street, Boston, MA 02115. Phone: 617-732-5500 x1401; FAX: 617-278-6957; E-mail: colgan@zeus.bwh.harvard.edu

Received for publication 18 March 1998 and accepted in revised form 29 July 1998.

J. Clin. Invest.

0021-9738/98/09/1161/12 $2.00
Volume 102, Number 6, September 1998, 1161–1172
http://www.jci.org

1. *Abbreviations used in this paper:* COX, cyclooxygenase; EDS, endothelial-derived secretagogue; HUVEC, human umbilical vein endothelial cells; ΔIsc, change in short circuit current; PGHS-1, prostaglandin H synthase-1, COX-1; PGHS-2, prostaglandin H synthase-2, COX-2.

forskolin (Sigma). NS398, PGE_2, and 2,3-dinor-keto-$PGF_{1\alpha}$ were purchased from Biomol Inc. (Plymouth Meeting, PA) or from Oxford Biomedical Research, Inc. (Oxford, MI). Ciprostene, 6-keto-$PGF_{1\alpha}$, and carbaprostacyclin were purchased from Cayman Biochemical (Ann Arbor, MI). 1,2-bis(2-aminophenoxy)ethane-*N*,*N*,*N*′,*N*′-tetraacetic acid (BAPTA 2-AM) was purchased from Molecular Probes (Eugene, OR). Iloprost was a kind gift from Schering Plough Inc. (Berlin, Germany).

Cell culture

Human umbilical vein endothelial cells (HUVEC). HUVEC were obtained and harvested using 0.1% collagenase (Worthington Biochemical Corp., Freehold, NJ) as described elsewhere (8). Endothelial monolayers were established and maintained on 9.5- or 1.9-cm^2 gelatin-coated plates using DME (Gibco, Grand Island, NY) containing 10% heat-inactivated FCS, glucose, pyruvate, glutamine, and streptomycin (9). Confluent monolayers exhibited typical cobblestone appearance. Where indicated, confluent monolayers were exposed to activating conditions (LPS, IL-1α, or TNF-α) as described before (9). In subsets of experiments, serum-starved endothelia (12 h) were exposed to hypoxia (pO_2 20 mmHg) as previously reported (9, 10).

Human intestinal epithelial cell line (T84 cells). Monolayers of T84 cells (passages 67–85) were grown and passaged as previously described (11) in a 1:1 mixture of DME and Hams F-112 medium supplemented with 15 mM Hepes buffer (pH 7.5), 14 mM Na HCO_3, 40 mg/liter penicillin, 8 mg/liter ampicillin, 9 mg/liter streptomycin, and 5% FCS. Subculturing was performed every 6–8 d by treating with trypsin (0.1%) and EDTA (0.9 mM) in Ca^{2+} and Mg^{2+}-free PBS for 15–20 min.

For coculture experiments, two systems were developed to study endothelial influences on epithelial function (see Fig. 1). In system A, T84 cells were grown on the underside permeable supports as described previously (12). Once confluent, HUVEC were plated in the upper chamber of the collagen-coated insert and allowed to grow to confluency for 48 h before activation. This orientation provided particularly close endothelial–epithelial proximity, without allowing cell–cell contact (cells do not penetrate 0.4-μm filters, data not shown). In system B (Fig. 1), T84 cells were grown to confluence on the upperside of 0.4-μm permeable supports (Corning Costar, Cambridge, MA) and HUVEC were plated and grown to confluence in the opposing well before activation. Thus, development of these systems provided an opportunity to study paracrine crosstalk between endothelia and epithelia.

Electrophysiologic measurements

To measure agonist-stimulated short circuit currents (Isc), transepithelial potentials, and resistance, a commercially available voltage clamp (Iowa Dual Voltage Clamps, Bioengineering, University of Iowa) interfaced with an equilibrated pair of calomel electrodes and a pair of Ag-AgCl electrodes was used, as described in detail elsewhere (11). Using these values and Ohm's law, transepithelial resistance and transepithelial current were calculated. Fluid resistance within the system accounts for $< 5\%$ of total transepithelial resistance. HBSS was used in both apical and basolateral baths during all experiments, unless otherwise noted. Cl^- secretory responses are expressed as a change in short circuit current (ΔIsc) necessary to maintain zero potential difference across the monolayer.

Fluid transport assay

T84 cells growing on inserts were exposed to HUVEC or HUVEC media with or without LPS for 24 h, as indicated. Using system B (Fig. 1), net fluid movement was measured as described previously (13), with minor modifications. In brief, the apical solution of confluent T84 cell monolayers grown on 0.33-cm^2 permeable supports was replaced with 30 μl of media and layered with 60 μl of warm, sterile mineral oil to minimize evaporation as previously described (14). In some monolayers, the cAMP agonist forskolin (50 μM) and 3-isobutyl-1-methylxanthine (IBMX 100 μM) were added to the basolateral solution to promote fluid movement and serves as a positive control. After 24 h, the apical solution was collected, centrifuged at 10,000 *g*, and quantified with a calibrated pipette and weighed on a balance (Sartorius, Inc., Bohemia, NY).

Prostaglandin H synthase-1 (PGHS-1) and PGHS-2 Western blotting

HUVEC were grown to confluence on 6-well plates and exposed to experimental conditions (media alone or media containing 30 ng/ml IL-1α for 18 h). Washed monolayers were lysed (150 mM NaCl, 25 mM Tris, 1 mM $MgCl_2$, 1% Triton X-100, 1% Nonidet P-40, 5 mM EDTA, 5 μg/ml chymostatin, 2 μg/ml aprotinin, and 1.25 mM PMSF, all from Sigma) and cell debris was removed by centrifugation (10,000 *g*, 5 min). Cell lysates were separated by nonreducing SDS-PAGE, transferred to nitrocellulose, and blocked overnight in blocking buffer (250 mM NaCl, 0.02% Tween 20, 5% goat serum, and 3% BSA). Primary antibody to PGHS-1 (1:1,000 rabbit polyclonal) or PGHS-2 (1:1,000 rabbit polyclonal, both from Oxford Biomedical Research, Inc.) was added for 3 h, blots were washed, and species-matched peroxidase-conjugated secondary antibody was added. Labeled bands from washed blots were detected by ECL (Amersham, Inc., Arlington Heights, IL) as described before (10).

Isolation and identification of EDS

Conditioned media from HUVECs with and without stimulation were passed through a series of progressively smaller filters (10-, 3-, 1-, and 0.5-kD molecular mass cutoff; Amicon, Danvers, MA) under N_2 pressure, as described previously (15). Filter flow-through samples and filter retentates (volume adjusted back to original volumes) were tested by addition of samples to virgin T84 monolayers and assessment of electrogenic Cl^- secretion, as described above. Preconditioned media filtered through a 0.5-kD Amicon filter and pH adjusted to 3.5 were run across a Sep-Pak C_{18} column (Millipore Corp., Milford, MA). The columns were washed with distilled/deionized water and compounds were eluted with increasingly polar mobile phases (hexane→methyl formate→methanol), as described previously (16). Fractions were concentrated under a stream of nitrogen, reconstituted in either 1 ml of $HBSS^+$ (for T84 bioactivity) or 100 μl of methanol (for UV-HPLC-mass spectrometry). Active fractions from Sep-Pak were further resolved on a C_{18} reverse-phase HPLC column (150 × 5 mm; Phenomenex, Torrance, CA) with acidified (0.1% acetic acid) MetOH/H_2O (60:40 vol/vol) at 1 ml/min on a 1050 series HPLC using ChemStation™ software (Hewlett Packard, Palo Alto, CA). Eluted samples (1 ml) were trapped on a fraction collector (BioRad, Hercules, CA), evaporated to dryness, and resuspended in 1 ml HBSS for assay of bioactivity.

For structural elucidation of EDS, bioactive materials eluted by HPLC were injected into a liquid chromatograph in tandem with a mass spectrometer (LC/MS) using an ODS Hypersil column (Hewlett Packard) 2.1 × 100 mm. The LC/MS was run at 0.5 ml/min. Buffers were A = water with 0.1% formic acid, B = acetonitrile with 0.1% formic acid, with gradient set at 20.5% B to 75% B in 35 min using buffer A as a diluent. The mass spectrometer used was a Platform II (Micromass Instruments, Beverly, MA) operated using atmospheric pressure chemical ionization and operated such that scans of opposite polarity were obtained on alternating scans (alternating positive/negative ion mode). The instrument was scanned from mass 100 to 600 in 1 s, with a 0.1 interscan time. In this manner, full positive and negative ion mass spectra were obtained from a single chromatographic analysis.

In subsets of experiments, quantification of 6-keto-$PGF_{1\alpha}$ was performed using a commercially available ELISA kit (Oxford Biomedical Research, Inc.). For such analysis, 6-keto-$PGF_{1\alpha}$ was extracted from soluble supernatant using methyl formate elution from C_{18} Sep-Pak columns, evaporated to dryness, and resuspended in dilution buffer provided by the ELISA kit.

Intracellular signaling studies

In subsets of experiments, intracellular cAMP or cGMP was quantified exactly as described previously (17). In brief, confluent T84 monolayers on 5-cm^2 permeable supports were exposed to indicated experimental conditions and cooled to 4°C by washing in ice-cold HBSS. Cyclic nucleotides were extracted from washed monolayers with extraction buffer (1 ml of 66% EtOH, 33% HBSS containing the phosphodiesterase inhibitor IBMX, 5 mM, Sigma), lysates were cleared by spinning at 10,000 *g* for 5 min, and dried under vacuum to remove EtOH. Samples were rehydrated in water, and cyclic nucleotides were quantified using displacement ELISA (Amersham) according to manufacturer's instructions. Nucleotide levels were expressed as pM per ml of lysis buffer.

Ca^{2+} signaling was quantified exactly as described previously (18). In brief, T84 cells were grown on acid-washed, collagen-coated glass coverslips. Cells were grown subconfluent (to allow basolateral access of agonist), washed in warm HBSS, and loaded with the radiometric Ca^{2+} indicator fura 2-AM (Molecular Probes, final concentration of 7.5 μM) for 1 h at room temperature. Elevation in intracellular Ca^{2+} in response to agonist was assessed using a microscopic dual wavelength spectrofluorometer (model 4000; Photon Technology Int., South Berwick, NJ). Fura 2-AM was monitored at excitation wavelengths 340 and 380 nm and emission spectra were collected at 510 nm; the ratio of 340:380 nm accurately reflects intracellular Ca^{2+} (19). Results are expressed as the fluorescence ratio at wavelengths 340/380 nm. In subsets of experiments, inhibition of intracellular Ca^{2+} signaling was achieved by preexposure of epithelia to the Ca^{2+} chelator BAPTA 2-AM (100 μM, 10 min) before addition of agonist, as described previously (20).

Data presentation

Electrophysiologic, fluid transport and cAMP data were compared by two-factor ANOVA or by Student's *t* test where appropriate. Values are expressed as the mean±SEM of *n* monolayers from at least three separate experiments.

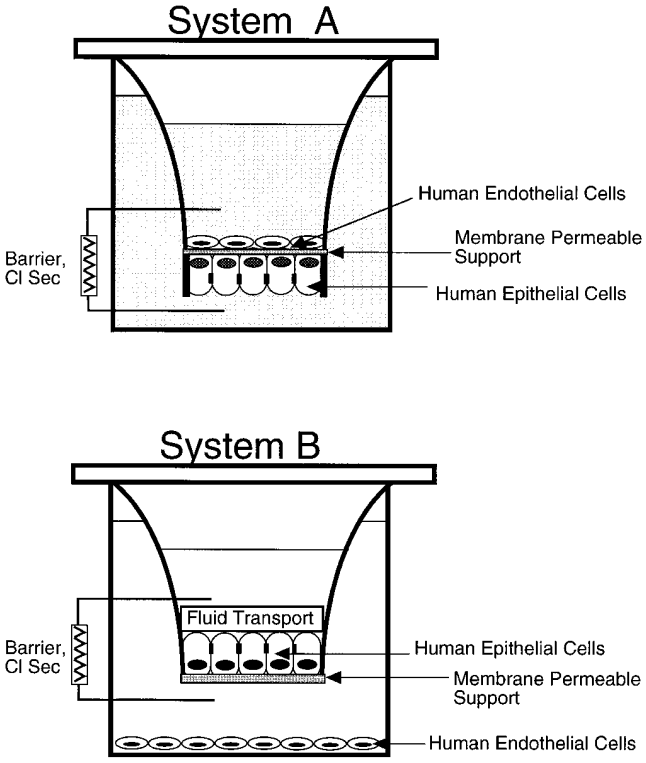

Figure 1. Systems of noncontact endothelial–epithelial cocultures. T84 intestinal epithelial monolayers were grown in noncontact coculture with HUVEC as described in Methods. In system A, epithelia and endothelia were plated on opposing surfaces of membrane-permeable supports. In system B, epithelia were plated on membrane-permeable supports whereas endothelia were plated in the adjacent well to the permeable support.

Results

Active endothelial–epithelial cocultures. Fig. 1 demonstrates the systems used to examine paracrine crosstalk between endothelia and epithelia. After plating in coculture, neither system (A nor B) resulted in significant differences in cell viability (based on LDH release from individual cell types and in coculture, data not shown). Additionally, the presence of endothelia did not influence epithelial barrier function, a sensitive measure of epithelial viability (11) (measured as a transepithelial resistance, 1,118±210 and 1,218±195 ohm · cm^2 for epithelia plated alone and in coculture with endothelia for 3 d [pooled for systems A and B], respectively, $n = 32$ monolayers per condition, P = not significant). HUVEC plated alone did not support a measurable resistance (data not shown).

We next examined functional epithelial endpoints of endothelial activation. As shown in Fig. 2 *A*, addition of LPS to endothelial–epithelial cocultures (system A, see Fig. 1) resulted in a time-dependent increase in epithelial Isc (measured as ΔIsc, $P < 0.01$ by ANOVA), indicating activation of epithelial electrogenic chloride secretion (11). Such responses were evident by 6 h ($P < 0.05$), maximal by 12 h, and remained significantly elevated out to 24 h. Over this same time course, cocultures incubated in the absence of LPS also revealed a small increase in Cl^- secretion over epithelia alone (Fig. 2 *A*, $P < 0.05$ compared with epithelia alone by ANOVA). Consistent with previous reports (21), LPS did not influence Cl^- secretory responses of epithelia alone. As shown in Fig. 2 *B*, we extended these data to examine the endpoint functional response of epithelial electrogenic chloride secretion, that of vectorial fluid transport (1). To do this, cocultures grown adjacent to one another (system B, Fig. 1) served as a better system since accurate quantification of fluid transport requires minimal epithelial apical volumes (13). As shown in Fig. 2 *B*, cocultures activated with LPS resulted in increased fluid transport over control cocultures (i.e., no LPS, 11±0.4-fold increase with LPS activation, $P < 0.005$) or epithelia alone (9±0.8-fold increase with coculture LPS activation, $P < 0.01$). As we have demonstrated previously (13), activation of epithelia with forskolin (50 μM) served as a positive control for this response (16±1.4-fold increase over epithelia alone, $P < 0.001$). Such data reveal that endothelial exposure to LPS in proximity to epithelia results in activation of Cl^- secretion and concomitant vectorial fluid transport.

Activated endothelia liberate a soluble secretagogue. We next determined whether induction of Cl^- secretion by activated endothelia (see Fig. 2) resulted from endothelial liberation of a soluble factor. To do this, conditioned media supernatants were harvested from LPS-stimulated endothelia (500 ng/ml, 18 h of exposure) and were incubated with quiescent epithelial monolayers. As shown in Fig. 3 *A*, epithelial exposure to conditioned media derived from activated endothelia resulted in a rapid rise in Isc (maximal by 3 min) which persisted over time (ΔIsc significantly higher than buffer alone at 40 min, $P <$

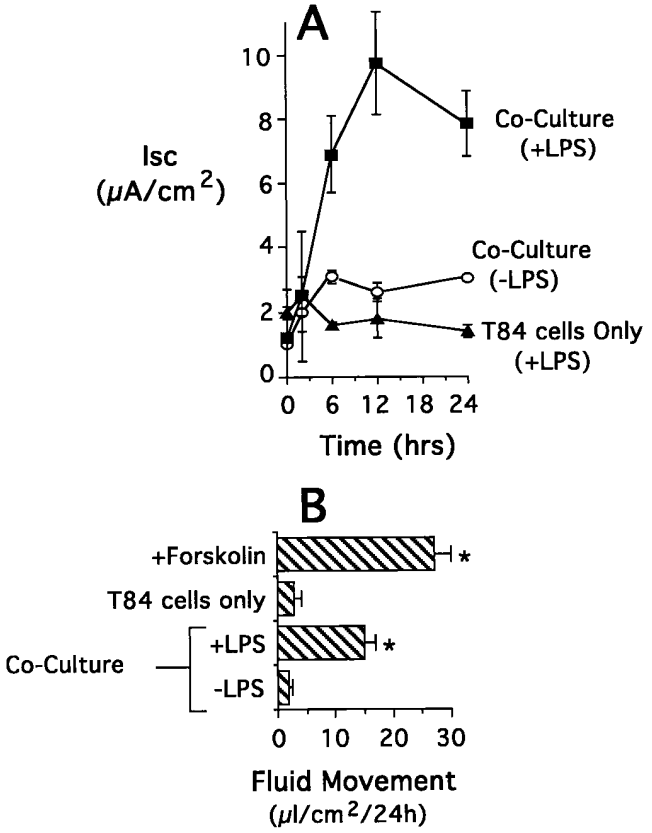

Figure 2. Induction of electrogenic Cl^- secretion and fluid transport in LPS-activated endothelial–epithelial cocultures. In *A*, system A cocultures were incubated in the absence (*open circles*) and presence of LPS (100 ng/ml, *closed squares*) for indicated times and examined for generation of epithelial electrogenic Cl^- secretion (measured as Isc). T84 monolayers alone (*closed triangles*) were incubated with LPS as a control. Results represent data pooled from eight monolayers in each condition and are expressed as the mean±SEM. In *B*, system B cocultures were incubated in the presence and absence of LPS (100 ng/ml) for 24 h and examined for vectorial basolateral-to-apical fluid transport as described in Methods. T84 cells alone served as a negative control and T84 cells exposed to forskolin (10 μM) in the presence of IBMX (5 mM) served as the positive control for induction of fluid transport. Data are pooled from eight monolayers in each condition and results are expressed as the mean±SEM fluid movement over 24 h.

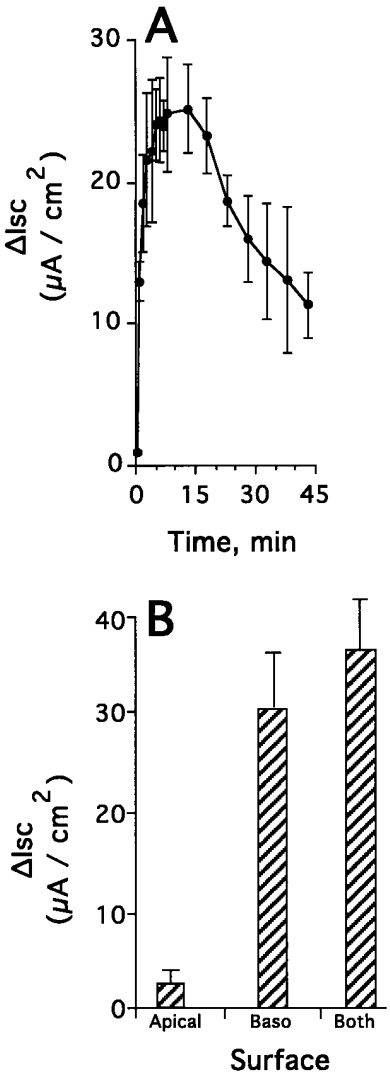

Figure 3. Conditioned media from LPS-activated endothelia induce epithelial Cl^- secretion. In *A*, supernatants harvested from LPS-activated endothelia (100 ng/ml, 18 h) were exposed to the basolateral surface of confluent T84 monolayers and examined for generation of electrogenic Cl^- secretion at indicated times. Data are pooled from eight monolayers in each condition and results are expressed as the mean± SEM ΔIsc. (*B*) Supernatants harvested from LPS-activated endothelia (100 ng/ml, 18 h) were exposed to the apical, basolateral, or apical and basolateral surfaces of confluent T84 cell monolayers and examined for generation of electrogenic Cl^- secretion. Data are pooled from nine monolayers in each condition and results are expressed as the mean±SEM ΔIsc.

0.05). The functional receptor for this secretagogue localized to the physiologically relevant basolateral surface. Indeed, as shown in Fig. 3 *B*, no significant increase in Isc was observed when soluble supernatants from LPS-activated endothelia were applied to the apical surface of epithelia (3.1±1.4 μA/cm^2 at 3 min after addition), whereas a vigorous response was obvious upon application to the basolateral surface (30.2±7.2 μA/cm^2 at 3 min after addition) or to both the basolateral and apical surfaces of confluent epithelia grown on permeable supports (36.1±6.6 μA/cm^2 at 3 min after addition). Such data indicate that activated endothelia liberate a soluble factor which when exposed to the epithelial basolateral membrane activates a rapid and sustained electrogenic Cl^- secretory response.

Activation dependence. We next examined the diversity of endothelial-activating stimuli for liberation of this soluble secretagogue. As shown in Fig. 4 *A*, conditioned media harvested from LPS-activated endothelia revealed a concentration-dependent increase in epithelial Isc (EC_{50} = 80 ng/ml, $P < 0.01$ by ANOVA). Higher concentrations of LPS (up to 1 μg/ml) did not result in enhanced liberation of this soluble factor (data not shown). Similarly, a time course of LPS activation (500 ng/ml) revealed a time-dependent increase in liberation of EDS (ΔIsc of 3.2±0.4, 6.6±0.6, 19.1±4.0, and 17.6±4.4 μA/cm^2 at 6, 12, 18, and 24 h of exposure to LPS, respectively, $P <$ 0.01 by ANOVA). Parallel supernatants harvested from unactivated endothelia revealed smaller increases in Isc (maximal ΔIsc = 3.3±0.6 μA/cm^2 at 18 h, $P < 0.05$ compared with media controls). Media harvested from epithelia alone or LPS-activated epithelia (Fig. 4) revealed no significant secretagogue activity (P = not significant compared with unconditioned media). Additionally, increased Isc responses were obtained from supernatants derived from endothelia stimulated with IL-1α (Fig. 4, EC_{50} = 1 ng/ml, $P < 0.01$ by ANOVA), TNF-α (EC_{50} = 25 ng/ml, maximal ΔIsc of 27.3±6.4 μA/cm^2 at 18 h, $P < 0.001$ compared with media control). Endothelial cell exposure to hypoxia (pO_2 20 torr, for periods of 12–48 h) (9, 10) also elicited liberation of secretagogue activity (ΔIsc of 8.4±1.7, 9.8±1.6, and 10.3±1.9 μA/cm^2 for periods of hypoxia of 12, 24,

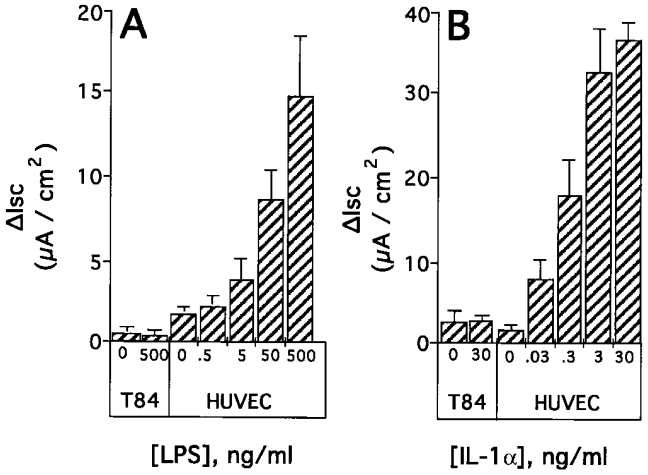

Figure 4. Diversity of activators for endothelial liberation of soluble secretagogue. Soluble supernatants were harvested from endothelia activated with indicated concentrations of LPS (18-h exposure, *A*) or IL-1α (18-h exposure, *B*). Supernatants were exposed to the basolateral surface of confluent T84 cell monolayers and examined for generation of electrogenic Cl^- secretion. Supernatants harvested from T84 cells exposed to LPS (500 ng/ml, *A*) or IL-1α (30 ng/ml) served as controls for these experiments. Data are pooled from 8–12 monolayers in each condition and results are expressed as the mean±SEM ΔIsc.

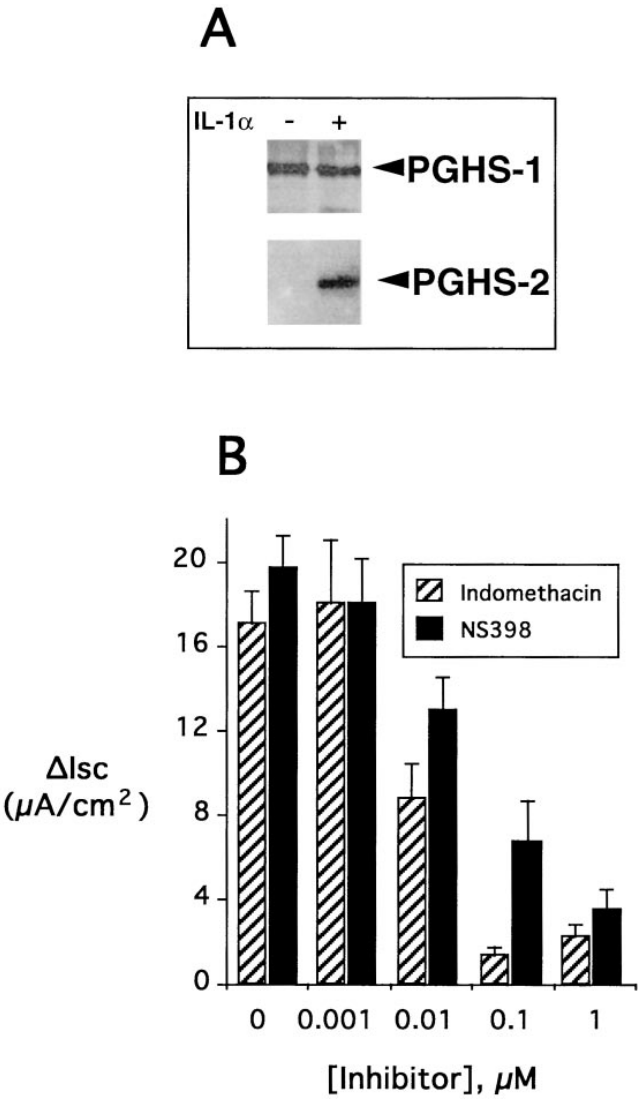

Figure 5. EDS activity parallels PGHS-2 (COX-2) induction. (*A*) Confluent endothelial monolayers were incubated in the presence and absence of IL-1α (30 ng/ml) for 18 h. Cells were cooled to 4°C, scraped, and solubilized as described in Methods. Lysates were separated by SDS-PAGE under nonreducing conditions, blots were probed with polyclonal rabbit anti–PGHS-1 (*top*) or PGHS-2 (*bottom*), labeled with peroxidase-conjugated secondary antibody, and developed by ECL. One of three representative experiments is shown. (*B*) Soluble supernatants were harvested from endothelia activated with IL-1α (3 ng/ml, 18 h) in the presence and absence of indicated concentrations of indomethacin (*hatched bars*) or NS398 (*solid bars*). Resulting supernatants were exposed to the basolateral surface of confluent T84 cell monolayers and examined for generation of electrogenic Cl^- secretion. Data are pooled from three separate experiments tested on seven to nine monolayers in each condition and results are expressed as the mean±SEM ΔIsc.

and 48 h, respectively, all are $P < 0.01$ compared with media control of 1.83±0.27, $n = 3$).

This Cl^- secretory response was not related to LPS, TNF-α, or IL-1α activation of T84 cells, since direct addition of these activators failed to induce significant Cl^- secretion [ΔIsc of 0.2±0.03, 1.2±0.7, 0.9±0.03 μA/cm² for LPS (500 ng/ml), TNF-α (50 ng/ml) or IL-1α (30 ng/ml), P = not significant compared with media alone]. Such data are consistent with previous studies indicating that in the baseline state, T84 cells do not express functional receptors for these inflammatory mediators (13, 22–24). Dilution of supernatant harvested from maximally activated endothelia (IL-1α, 3 ng/ml, 18 h) indicated a complete loss of activity at 1:25 dilution (37.4±5.1 vs. 1.1±0.5 μA/cm² for neat vs. 1:25 dilution, respectively, $P <$ 0.01). Such data indicate that endothelia, and particularly activated endothelia, liberate an epithelial Cl^- secretagogue (hereafter referred to as EDS).

Liberation of EDS requires cyclooxygenase-2 (COX-2) activity. We next attempted to block production of EDS. First, as shown in Fig. 5 *A*, conditions for liberation of EDS paralleled induction of PGHS-2 (COX-2) but not PGHS-1 (COX-1). Western blotting of endothelial lysates under conditions which liberate this secretagogue (IL-1α, 30 ng/ml, 18 h, see Fig. 4) revealed a dominant increase in COX-2, with stable expression of COX-1. Such data are consistent with previous reports of COX-2 as an inducible enzyme in endothelia (25, 26). Moreover, as shown in Fig. 5 *B*, pretreatment of endothelia with either indomethacin (more selective inhibitor of COX over lipoxygenases) (27) or NS398 (more selective inhibitor of COX-2 over COX-1) (28) blocked IL-1α–activated liberation of this secretagogue bioactivity by > 90%. Such inhibition of EDS responses was not a result of indomethacin or NS398 action on T84 cells, since neither inhibited EDS-elicited Cl^- secretion in epithelia (ΔIsc 12.2±2.5 and 13.7±3.1 for EDS with 1 μM indomethacin or NS398, respectively, vs. 14.2±3.0 and 12.6±0.5 for EDS alone, respectively, $n = 3$ separate experiments, P = not significant). Taken together, these data indicate that EDS liberation parallels COX-2 induction.

Structural nature of endothelial secretagogue. Data presented above revealed that EDS is liberated into supernatants, is stable as a soluble factor, and may require COX-2 induction. To

gain further insight into the nature of EDS, we examined a number of physical parameters. First, ultrafiltration of supernatants through progressively smaller membrane pore sizes (range 30–0.5 kD) revealed no loss of activity through filters as low as 500 D (bioactivity of 21.6±6.5.0 vs. 27.0±5.4 $\mu A/cm^2$ for unfiltered EDS and EDS filtered through a 500-D membrane filter, respectively, P = not significant). Additionally, EDS was demonstrated to resist multiple freeze/thaw cycles and could be lyophilized without loss of activity (data not shown). Such physical parameters strongly resembled that of an endogenous secretagogue (29), later identified as 5′AMP, which is converted to adenosine at the epithelial surface and stimulates epithelial A_{2b} receptors (15, 30). However, EDS bioactivity was not blocked by the addition of the adenosine receptor antagonist 8-phenyl-theophylline (19.0±6.3.9 vs. 17.2±6.4 $\mu A/cm^2$ in the presence and absence of 8-phenyltheophylline, respectively, P = not significant; whereas such conditions blocked 5 μM adenosine-stimulated Isc by 94±6%). Further experiments, shown in Fig. 6 *A*, revealed that EDS bound to C_{18} Sep-Pak columns and eluted within the methyl formate fraction. Repeated UV spectral scans of active, partially purified EDS (filtrate ≤ 500 D, eluted from C_{18} column with methyl formate, evaporated to dryness under N_2, and resuspended in methanol) failed to reveal an obvious chromophore within the range of 210–400 nm (data not shown).

Identification of EDS. As a starting point for structural elucidation of EDS, partially purified EDS (in methanol) was injected on a C_{18} reverse-phase HPLC column. Samples were eluted in MetOH/water (60:40 vol/vol) in 0.1% acetic acid mobile phase, collected as 1-ml fractions over 30 min, evaporated to dryness under N_2, resuspended in HBSS, pH adjusted to 7.4, and screened for induction of epithelial Cl^- secretion. Shown in Fig. 6 *B* are bioactivities of fractions 4–12 min which revealed highly active fractions eluting at 8–11 min. Samples in the 1–4 min and 13–30 min ranges did not significantly induce epithelial Cl^- secretion (not shown). Similar preparations of identically treated media controls revealed no observable bioactivity (maximum ΔIsc of 0.3±0.05 $\mu A/cm^2$, P = not significant compared with HBSS alone).

We next used LC/MS to obtain evidence for the structure of EDS. As shown in Fig. 7 *A*, in the negative ion mode, endogenous EDS revealed a single dominant total ion peak (Fig. 7 *A*, *inset*) and a dominant ion at $[M - H]^-$ at *m/z* 369, providing evidence for M = 370. Very little fragmentation was evident, and those evident were indicative of successive water losses 351 $[M - H_2O]^-$, 333 $[M - 2H_2O]^-$, and 315 $[M - 3H_2O]^-$. By contrast, positive ion mass spectra (Fig. 8 *A*) revealed a single dominant total ion peak (Fig. 8 *A*, *inset*) with significant fragmentation at *m/z* 393 $[M + Na]^+$, and loss of successive water molecules from the putative protonated molecule, 353 $[M - H_2O]^+$, 335 $[M - 2H_2O]^+$, and 317 $[M - 3H_2O]^+$. Given that EDS resembles a prostanoid or eicosanoid generated through the COX-2 induction pathway (Figs. 5 and 6), the best candidate with M = 370 was 6-keto-$PGF_{1\alpha}$, an hydrolysis product of PGI_2 (31, 32). The negative and positive ion spectra for 6-keto-$PGF_{1\alpha}$ are shown in Figs. 7 *B* and 8 *B*, respectively. As can be seen, LC/MS characteristics of EDS and 6-keto-$PGF_{1\alpha}$ were essentially identical, and coinjection of EDS with synthetic 6-keto-$PGF_{1\alpha}$ (50% EDS and 50% 6-keto-$PGF_{1\alpha}$) revealed similar retention times (Figs. 7 *C* and 8 *C*, *insets*) and similar mass spectra (Figs. 7 *C* and 8 *C*), identifying EDS as 6-keto-$PGF_{1\alpha}$.

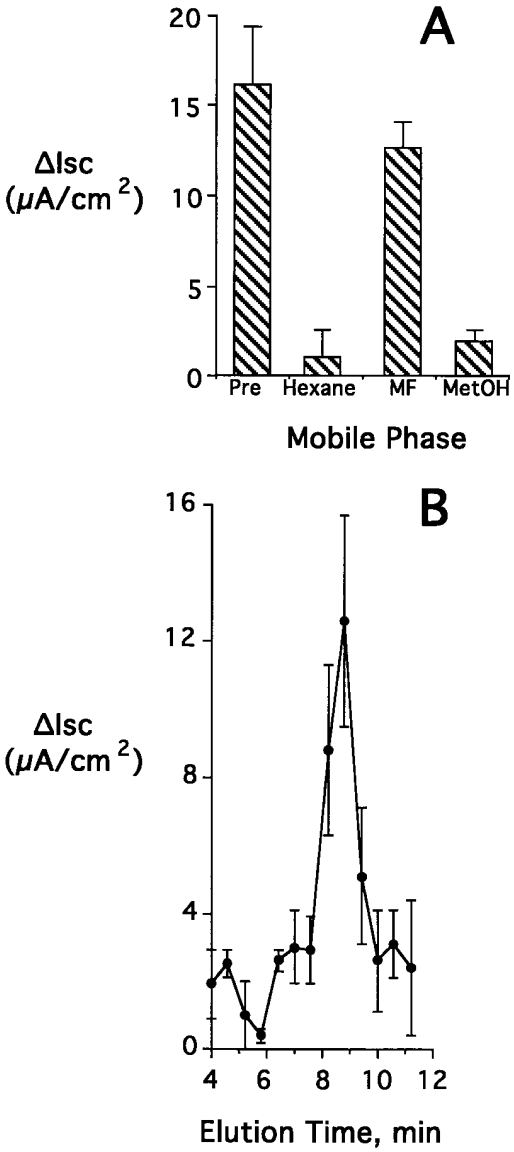

Figure 6. Purification of bioactive EDS. Soluble supernatants were harvested from endothelia activated with IL-1α (30 ng/ml, 18 h). In *A*, 3 ml of filtered supernatant (< 500 D) was passed across a C_{18} Sep-Pak column, washed with H_2O, and eluted with hexane, methylformate (*MF*), or methanol (*MetOH*) mobile phases. Column eluents were dried, resuspended in HBSS, exposed to the basolateral surface of confluent T84 cell monolayers, and examined for generation of electrogenic Cl^- secretion. Pre-C18 column supernatant (1 ml) served as a control. Data are pooled from 8–12 monolayers in each condition and results are expressed as the mean±SEM ΔIsc. (*B*) Samples derived from the methylformate fraction from C_{18} Sep-Pak columns were further separated by HPLC as described in Methods and tested for generation of electrogenic Cl^- secretion. Data are pooled from six to eight monolayers in each condition and results are expressed as the mean±SEM ΔIsc.

To verify the existence of 6-keto-$PGF_{1\alpha}$ in this model, supernatants derived from maximally activated endothelia were analyzed using a specific ELISA. Analysis of extracted soluble supernatants from endothelia preexposed to LPS (500 ng/ml, 18 h), TNF-α (50 ng/ml, 18 h), IL-1α (30 ng/ml, 18 h), or ambient cellular hypoxia (pO_2 20 torr, 48 h) revealed soluble

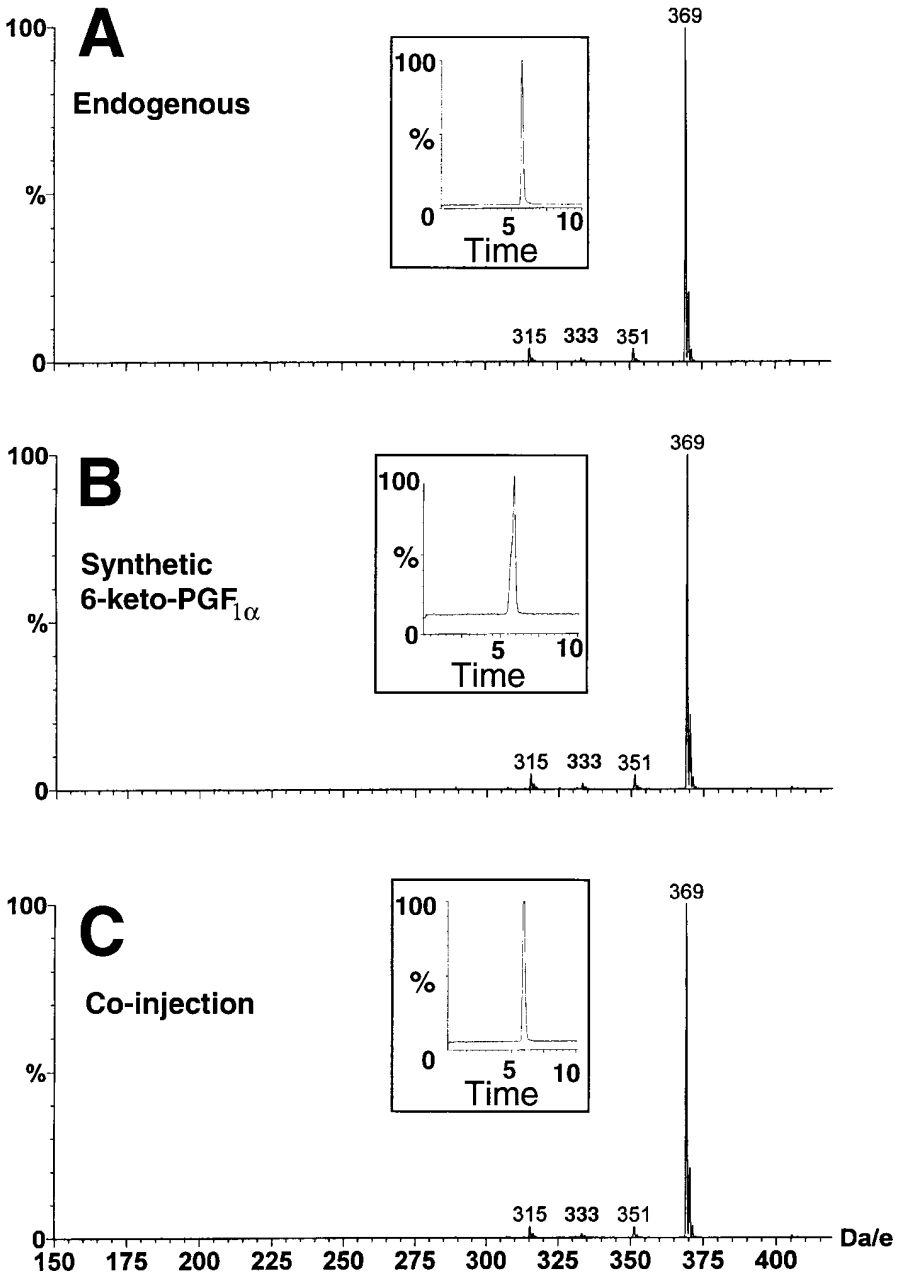

Figure 7. Negative ion mass spectral analysis of EDS and synthetic 6-keto-$PGF_{1\alpha}$. HPLC-purified EDS was analyzed by LC/MS as described in Methods. Shown here are representative mass spectral tracings in the negative ion mode and total ion elutions over the 10-min period of monitoring (*insets*). *A* represents endogenous EDS derived from endothelial supernatant partially purified by HPLC. *B* represents synthetic 6-keto-$PGF_{1\alpha}$. *C* represents a coinjection of endogenous EDS and synthetic 6-keto-$PGF_{1\alpha}$.

6-keto-$PGF_{1\alpha}$ concentrations of 9.2±1.5, 13.2±3.4, 15.3±6.2, and 9.0±3.1 ng/ml, respectively (n = 3 separate experiments, all $P < 0.01$ compared with endothelial media alone). Importantly, media derived from endothelia not exposed to activating stimuli (18-h exposure) also had measurable amounts of 6-keto-$PGF_{1\alpha}$ (0.22±0.03 ng/ml, $P < 0.05$ compared with media alone). The addition of either indomethacin (1 μM) or NS398 (1 μM) blocked 6-keto-$PGF_{1\alpha}$ production by > 90% (soluble 6-keto-$PGF_{1\alpha}$ concentrations of 1.2±0.2 and 2.2±0.4 ng/ml for IL-1α–stimulated endothelia in the presence of indomethacin or NS398, respectively, $P < 0.01$ compared with levels derived from IL-1α–activated endothelia). Similar results were obtained with endothelia activated with other proinflammatory stimuli (77±4, 84±9, and 92±10% decrease in LPS, TNF-α, and hypoxia-stimulated 6-keto-$PGF_{1\alpha}$ levels with addition of 1 μM indomethacin, respectively, $P < 0.01$ for all).

Characteristics of a functional epithelial 6-keto-$PGF_{1\alpha}$ receptor. As an extension of the above defined data, we defined functional features of the epithelial 6-keto-$PGF_{1\alpha}$ receptor. In vivo, 6-keto-$PGF_{1\alpha}$ results from rapid hydrolysis of prostacyclin (PGI_2) (33) and in addition to 6-keto-$PGF_{1\alpha}$, 2,3-dinor-6-keto-$PGF_{1\alpha}$ is a major human metabolite of PGI_2 (34). Thus, as shown in Fig. 9, we compared relative bioactivities of 6-keto-$PGF_{1\alpha}$, 2,3-dinor-6-keto-$PGF_{1\alpha}$, and a panel of PGI_2 stable analogues (iloprost, carbaprostacyclin, and ciprostene, see structures in Fig. 9). Addition of synthetic 6-keto-$PGF_{1\alpha}$ to the basolateral surface of T84 epithelial monolayers induced a rapid and sustained Cl^- secretory response (ED_{50} = 80 nM, maximal ΔIsc 37.5±7.0 μA/cm^2 at 3 μM). The pattern of activation was similar to that of EDS (i.e., rapid and sustained, see Fig. 3) and the receptor was defined to the basolateral surface (i.e., apical addition of 6-keto-$PGF_{1\alpha}$ at concentrations up to

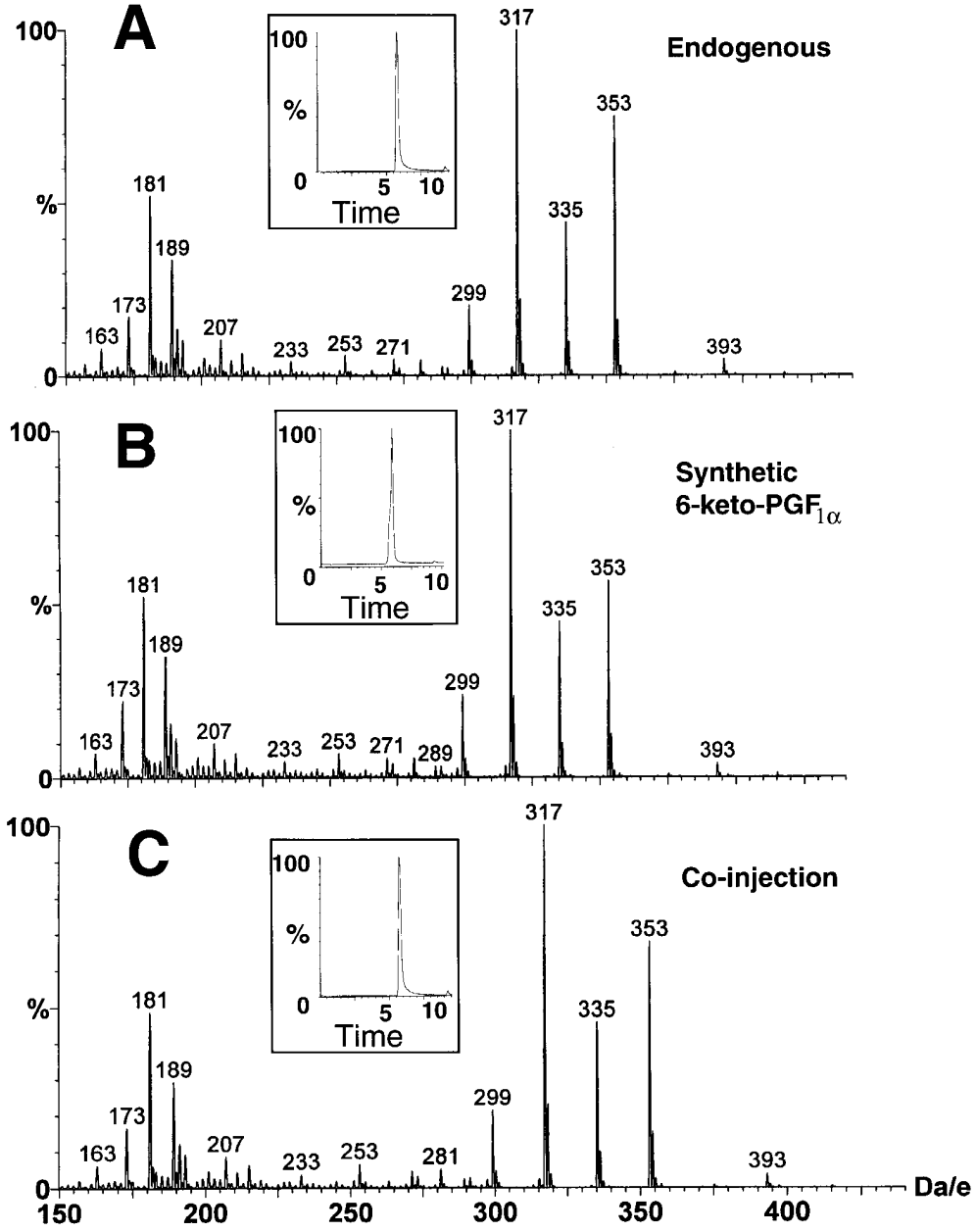

Figure 8. Positive ion mass spectral analysis of EDS and synthetic 6-keto-$PGF_{1\alpha}$. HPLC-purified EDS was analyzed by LC/MS as described in Methods. Shown here are representative mass spectral tracings in the positive ion mode and total ion elutions over the 10-min period (*insets*). *A* represents endogenous EDS derived from endothelial supernatant partially purified by HPLC. *B* represents synthetic 6-keto-$PGF_{1\alpha}$. *C* represents a coinjection of endogenous EDS and synthetic 6-keto-$PGF_{1\alpha}$.

3 μM did not induce an Isc, data not shown). Synthetic 6-keto-$PGF_{1\alpha}$ was more potent than the prostacyclin stable analogues carbaprostacyclin (ED_{50} = 180 nM, $P < 0.025$ compared with 6-keto-$PGF_{1\alpha}$), iloprost (ED_{50} = 240 nM, $P < 0.025$ compared with 6-keto-$PGF_{1\alpha}$), or ciprostene (ED_{50} = 280 nM, $P < 0.025$ compared with 6-keto-$PGF_{1\alpha}$). The synthetic 2,3-dinor-6-keto-$PGF_{1\alpha}$ compound was completely inactive at all concentrations examined (up to 3 μM, P = not significant compared with buffer controls). The 6-keto-$PGF_{1\alpha}$ response was less active than the related prostanoid PGE_2 (ED_{50} = 1 nM, $P < 0.001$ compared with 6-keto-$PGF_{1\alpha}$), which has been characterized previously in this model (35). As shown in Fig. 10, further experiments revealed it likely that 6-keto-$PGF_{1\alpha}$ acts through the PGI_2 receptor. Preexposure of epithelia to either 6-keto-$PGF_{1\alpha}$ or carbaprostacyclin results in attenuation of subsequent activation by carbaprostacyclin or 6-keto-$PGF_{1\alpha}$, respectively ($P < 0.025$ for both responses), suggesting classical receptor desensitization. Such attenuated responses were not a result of nonspecific signal uncoupling since carbachol, a Ca^{2+} agonist which does not activate the PGI_2 receptor, readily induced Cl^- secretion in desensitized monolayers (Fig. 10, $P < 0.001$ for both). Importantly, 6-keto-$PGF_{1\alpha}$ does not bind to the epithelial PGE_2 receptor, since epithelial preexposure to PGE_2 (100 nM, ΔIsc 38.6±4.2 μA/cm^2) did not attenuate subsequent responses to 6-keto-$PGF_{1\alpha}$ (100 nM, ΔIsc 22.6±3.1 μA/cm^2) compared with 6-keto-$PGF_{1\alpha}$ alone (100 nM, ΔIsc 23.0±4.7 μA/cm^2, P = not significant compared with combination of PGE_2 and 6-keto-$PGF_{1\alpha}$).

We next examined epithelial 6-keto-$PGF_{1\alpha}$ receptor coupling in intestinal epithelia. Previous studies have revealed that functional prostanoid receptors act through increased or decreased intracellular cAMP (36) or through elevations in intracellular Ca^{2+} (via IP_3 generation) (36). Thus, we examined intracellular cAMP responses to exogenous addition of 6-keto-

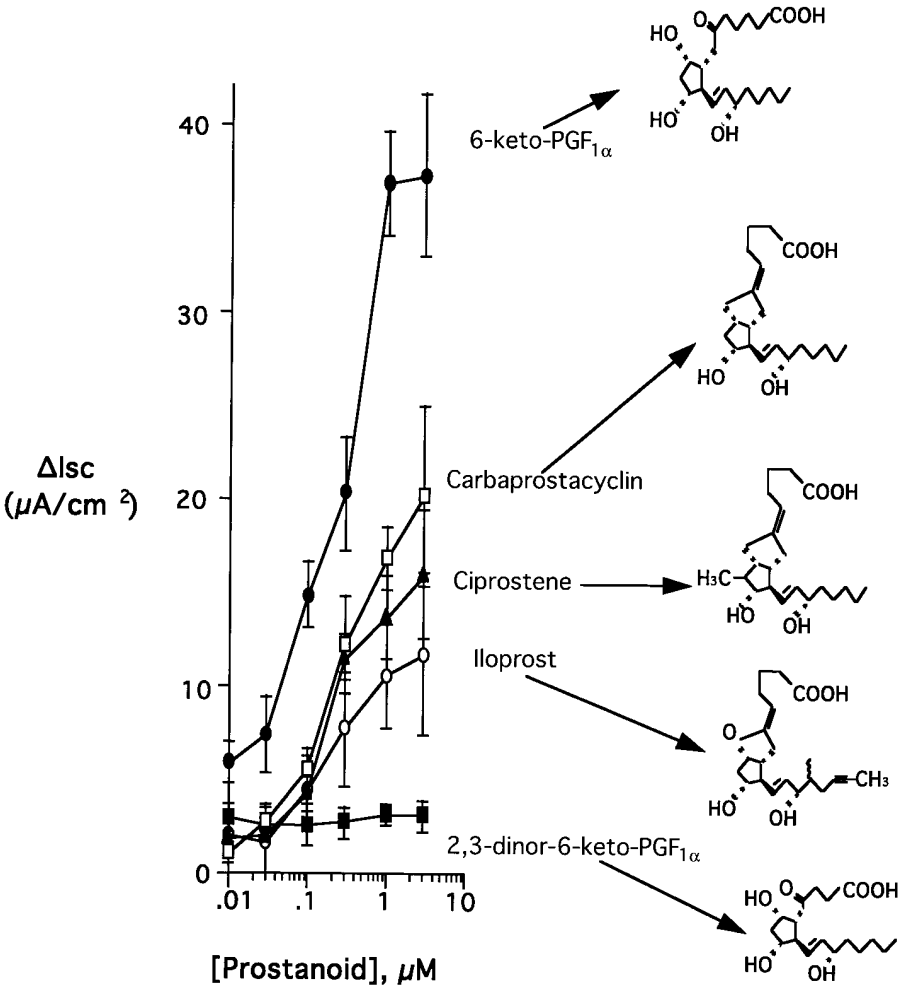

Figure 9. Comparison of synthetic 6-keto-$PGF_{1\alpha}$ and PGI_2 analogues in induction of epithelial electrogenic Cl^- secretion. Confluent T84 intestinal epithelial monolayers were exposed (basolateral only) to indicated synthetic PGs (structures of each are indicated) at indicated concentrations. Electrogenic Cl^- secretion was monitored over 30 min. Data are pooled from six to eight monolayers in each condition and results are expressed as the mean±SEM ΔIsc.

$PGF_{1\alpha}$ (basolateral exposure to 3 μM for 1–10 min). 6-keto-$PGF_{1\alpha}$ did not significantly elevate intracellular cAMP (98± 7% of vehicle control at 5 min, $n = 3$ separate experiments, P = not significant) compared with our positive control PGE_2 (3 μM, 184±10.9-fold increase over vehicle control at 5 min, $n = 3$ separate experiments, $P < 0.0001$), suggesting that the functional epithelial 6-keto-$PGF_{1\alpha}$ receptor is not coupled to cAMP-dependent processes. Parallel experiments revealed that 6-keto-$PGF_{1\alpha}$ did not elevate cGMP (data not shown). As shown in Fig. 10 *C*, stimulation of subconfluent (to allow basolateral access of agonist), fura 2-AM–loaded T84 cells with 6-keto-$PGF_{1\alpha}$ (1 μM) resulted in a rapid elevation in intracellular ionized Ca^{2+} (4.2-fold increase in 340/380 nm ratio). Histamine (100 nM, which elicits a ΔIsc of 47±8 μA/cm^2 at this concentration), an agonist which acts through elevation of intracellular Ca^{2+} (35), served as a positive control for these experiments (5.6-fold increase in 340/380 nm ratio), and 2,3-dinor-6-keto-$PGF_{1\alpha}$ did not elevate intracellular Ca^{2+}. Furthermore, pretreatment of epithelia with the intracellular $Ca2^+$ chelator BAPTA (100 μM, 10 min) resulted in a 51±4% decrease in -6-keto-$PGF_{1\alpha}$–induced Isc ($P < 0.05$ compared with no BAPTA). In parallel experiments, similar BAPTA treatment did not influence forskolin-stimulated Isc (12±5% decrease in Isc, P = not significant compared with no BAPTA). These data indicate the likelihood that the 6-keto-$PGF_{1\alpha}$ receptor is coupled through a Ca^{2+}-dependent pathway. Cumulatively, these results reveal that intestinal epithelia express a functional basolateral receptor for prostacyclin and 6-keto-$PGF_{1\alpha}$, the ligation of which results in a Ca^{2+}-dependent induction of electrogenic Cl^- secretion.

Discussion

In a number of conditions, including hemorrhagic shock, sepsis, and reperfusion injury, vascular endothelial activation parallels intestinal symptomologies consistent with epithelial electrogenic chloride secretion, namely secretory diarrhea (37–40). Such clinical observations implicate a role for endothelial-derived factor(s), at least in part, as mediators of such symptoms. In this study, we sought to elucidate the possible nature of these factor(s). As an experimental system, we used human cell cultures consisting of endothelial cells (HUVEC) plated in noncontact coculture with intestinal epithelia (T84 cells). Such cocultures revealed that endothelial-specific agonists liberate a soluble factor, which when applied to the basolateral surface of epithelia, induces a rapid and sustained Cl^- secretory response and concomitant fluid movement. Subsequent experiments identified this factor as 6-keto-$PGF_{1\alpha}$ and revealed that epithelia express a functional, basolateral cell surface receptor for both prostacyclin and 6-keto-$PGF_{1\alpha}$. This is the first evidence for a functional cellular response to 6-keto-$PGF_{1\alpha}$.

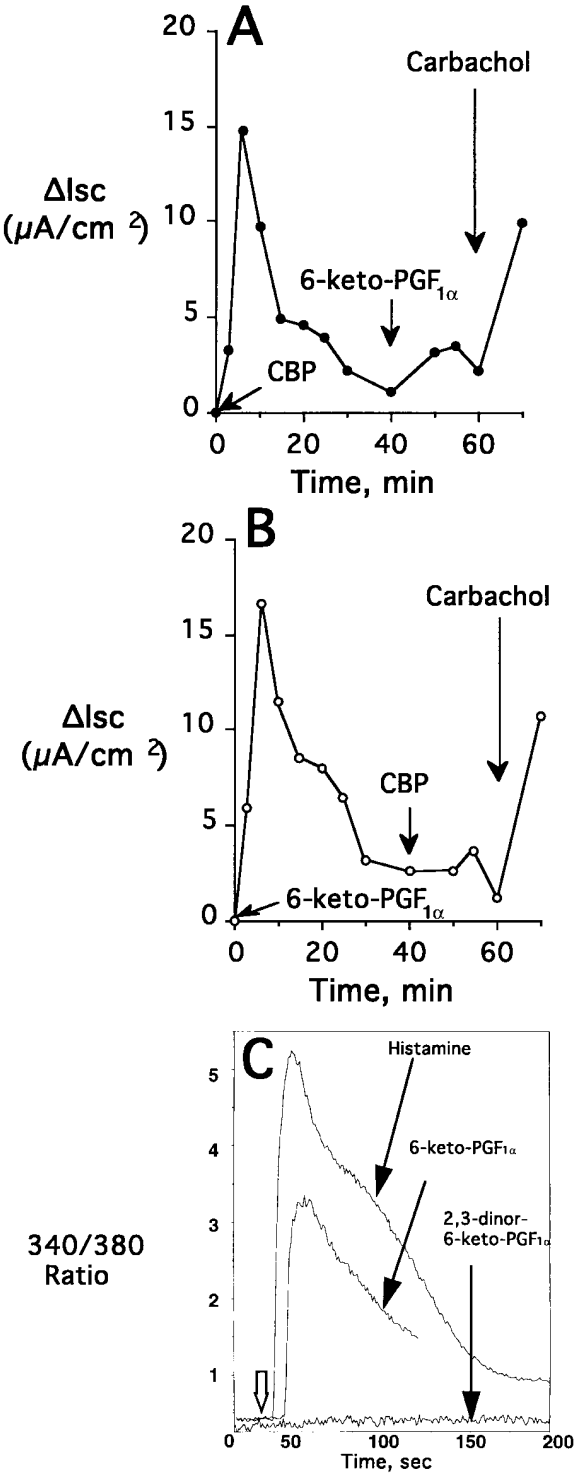

Figure 10. Characteristics of the epithelial 6-keto-$PGF_{1\alpha}$ receptor. (*A*) Confluent T84 intestinal epithelial monolayers were exposed (basolateral only) to synthetic carbaprostacyclin (*CBP*, 1 μM) followed by 6-keto-$PGF_{1\alpha}$ (1 μM) to examine receptor desensitization. The functional readout was induction of epithelial electrogenic Cl secretion. Carbachol (10 μM) was added at the end of the experiment to rule out nonspecific downregulation of calcium-stimulated Cl^- secretion. In *B*, T84 cells were exposed (basolateral only) to synthetic 6-keto-$PGF_{1\alpha}$ (1 μM) followed by carbaprostacyclin (*CBP*, 1 μM) to examine receptor desensitization. Data are pooled from six to eight monolayers in each condition and results are expressed as the mean±SEM ΔIsc. In *C*, fura 2-AM–loaded, subconfluent T84 cells (to allow basolateral access of agonist) were visualized by microscopy, exposed to 6-keto-$PGF_{1\alpha}$ (1 μM), histamine(100 nM), or 2,3-dinor-6-keto-$PGF_{1\alpha}$ (1 μM), and examined for elevation in intracellular Ca^{2+} (measured as a ratio of fluorescence intensity at 340/380 nm). Data are representative tracings from three separate experiments.

Mucosal epithelia which line organs such as the intestine and lung lie in close anatomic proximity to a number of subepithelial cell types, including vascular endothelia. As such, the activated endothelium can produce soluble mediators which influence epithelial function. In the intestine for instance, PGs are derived almost exclusively from subepithelial populations (4), and recent evidence directly implicates a protective role for PGI_2 and PGE_2 in intestinal epithelial responses to reperfusion injury (41). To model such cell–cell crosstalk in vitro, it was necessary to position endothelia in close proximity, but not in contact, with the epithelial basolateral membrane. Our studies revealed that activation of noncontact cocultures with endothelia-specific agonists (LPS) elicited epithelial electrogenic Cl^- secretion and concomitant fluid transport over a period of 24 h. These results parallel a previous coculture system using fibroblast–epithelial cultures to study agonist responsiveness in intestinal epithelia (42, 43). Similar to our findings, these studies determined a role for COX products, particularly PGE_2, and revealed that fibroblasts promote agonist-stimulated epithelial Cl^- secretion. Our studies revealed that activated endothelia liberate a small, stable secretagogue into conditioned media supernatants. Similar to other bioactive molecule receptors (e.g., cytokines), the receptor for EDS was expressed in the physiologically relevant basolateral surface (i.e., toward the vasculature in vivo).

A diverse panel of endothelial activators was able to induce liberation of this secretagogue into soluble supernatants. A well-characterized, inducible enzyme in endothelial cells is COX-2 (7), and liberation of EDS paralleled COX-2 induction in this system. First, stimuli used to activate release of EDS (LPS, TNF-α, IL-1α, cellular hypoxia) have each been demonstrated to induce COX-2 protein levels (6, 44) and the time course of action (i.e., > 6 h) corresponds to the lag phase of COX-2 previously observed (45). Second, use of preferential inhibitors to COX over lipoxygenases (indomethacin) and more specific inhibitors of COX-2 over COX-1 (NS398) revealed a > 90% inhibition of EDS liberation, suggesting a dominant role for COX-2. Third, the presence of both unactivated endothelial cells in coculture and conditioned media from unactivated endothelia induced a low level Cl^- secretory response over media alone, indicating the likelihood that quiescent endothelia also produce some bioactive 6-keto-$PGF_{1\alpha}$ in this system. Basal expression of COX-1 could explain such observations (see Results). Additionally, we cannot rule out the possible role for other endothelial-derived bioactive lipids within this system, particularly PGE_2, of which intestinal epithelia bear a functional receptor (35) (see Results). In fact, it is likely, that PGE_2 may contribute to our observed increases in Cl^- secretion and fluid transport, as others have revealed a dominant role for PGE_2 in epithelial–fibroblast coculture systems (42, 43), and T84 epithelial cells express an active PGE_2 receptor (35). 6-keto-$PGF_{1\alpha}$ levels in soluble supernatants were determined to be in the nanogram range, and based on the concentration–response curve, this concentration does not

fully explain the EDS response observed in these experiments. Thus, while 6-keto-$PGF_{1\alpha}$ contributes to this response, it is likely that other stable, COX-dependent, bioactive components contribute to the Cl^- secretory responses in this coculture model. The identities of these others are not fully understood at this time.

Of interest, we found that EDS was stable under the conditions defined here and transferable in a cell-free conditioned supernatant derived from activated endothelial monolayers. Structural studies revealed 6-keto-$PGF_{1\alpha}$ as a predominate EDS in this system. Previously, 6-keto-$PGF_{1\alpha}$ was assumed to be an inactive, nonenzymatic hydrolysis product of prostacyclin, an unstable prostanoid derived from the COXs (46). Given their stability under physiologic conditions, 6-keto-PGF compounds have been used extensively as a urinary marker of endothelial activation in vivo (47). For example, the fate of labeled prostacyclin in humans was examined and revealed that all identified metabolites were of the 6-keto-PGF structure (32). Of note, urinary 6-keto-$PGF_{1\alpha}$ constituted nearly 6% of systemically administered prostacyclin. Our present studies indicate that intestinal epithelia express functional surface receptors for 6-keto-$PGF_{1\alpha}$, the ligation of which results in induction of electrogenic Cl^- secretion. Importantly, 2,3-dinor-6-keto-$PGF_{1\alpha}$, the major metabolite of 6-keto-$PGF_{1\alpha}$ (34), was completely inactive, revealing a relative importance of carbon positions 2 and 3 in activating the cell surface receptor (see Fig. 9). Additionally, these experiments reveal that prostacyclin stable analogues activate Cl^- secretion in model intestinal epithelia. The rank order of potency (Fig. 9, carbaprostacyclin $\sim$ ciprostene $>$ iloprost) reveals that the methyl group at C-22 on iloprost may, by comparison with the other analogues, partially inhibit interaction with the epithelial receptor. At present, we do not know if other 6-keto-PGs are active in this system.

Several lines of evidence indicate that 6-keto-$PGF_{1\alpha}$ activates a PGI_2 receptor (likely the IP receptor), a recently cloned seven-transmembrane–spanning protein (48, 49). First, epithelial preexposure to the prostacyclin analogue carbaprostacyclin resulted in receptor desensitization to subsequent activation by 6-keto-$PGF_{1\alpha}$. Second, whereas iloprost has been demonstrated also to activate the PGE_2 receptor (specifically the EP_1 receptor) (36), PGE_2 did not desensitize subsequent activation by 6-keto-$PGF_{1\alpha}$ (see Results). Of note, it is possible that epithelial PGI_2 (IP) and PGE (EP_1) receptors share a common signaling pathway since, for example, oocytes expressing IP receptors display a Ca^{2+}-mediated Cl^- current, similar to our findings here (48, 49). Third, while most evidence indicates that the PGI_2 receptor signals through cAMP (36), the cloned mouse PGI_2 receptor (48) as well as the rabbit cortical collecting duct (50) also signal through intracellular phosphatidylinositol hydrolysis and elevations in intracellular Ca^{2+}. In addition, PG responses of porcine intestinal epithelia implicated a role for increased intracellular Ca^{2+} (41). Thus, our findings that an intestinal epithelial PGI_2 receptor signals (via 6-keto-$PGF_{1\alpha}$) through elevation in intracellular Ca^{2+} are not unprecedented in the literature.

In summary, these findings reveal a novel paracrine pathway for endothelial–epithelial crosstalk. Such results indicate that physiologically stable PGs (e.g., 6-keto-$PGF_{1\alpha}$) have the potential to activate adjacent cell types in a paracrine manner. Moreover, given its in vivo stability (e.g., remains structurally intact in both urine and serum) (32), 6-keto-$PGF_{1\alpha}$ could provide a previously undefined systemic prostanoid signaling pathway. Whether these in vitro observations can be extended to in vivo settings awaits further investigation.

Acknowledgments

The authors gratefully acknowledge insightful discussions with Dr. Charles N. Serhan, assistance with mass spectrometry from Dr. Andrew Tyler of the Harvard Mass Spectrometry Facility, and technical assistance from Ms. Margaret Morrisey and Ms. Nana Fueki.

This work was supported by National Institutes of Health (NIH) grants DK-50189 to S.P. Colgan, HL-52886 and HL-56086 to G.L. Stahl, DK-09699 to C.T. Taylor, and HL-03688 to P.F. Lennon. E.D. Blume was supported by NIH training grant HL-07572 to Children's Hospital of Boston.

References

1. Powell, D.W. 1987. Intestinal water and electrolyte transport. *In* Physiology of the Gastrointestinal Tract. L.R. Johnson, editors. Raven Press, New York. 1267–1291.

2. Powell, D.W. 1991. Immunophysiology of intestinal electrolyte transport. *In* Handbook of Physiology. American Physiological Society. 591–641.

3. Powell, D. 1981. Barrier function of epithelia. *Am. J. Physiol.* 241:G275–G288.

4. Lawson, L.D., and D.W. Powell. 1987. Bradykinin-stimulated eicosanoid synthesis and secretion of rabbit ileal components. *Am. J. Physiol. (Gastrointest. Liver. Physiol.).* 252:G783–G790.

5. Breider, M. 1993. Endothelium and inflammation. *JAVMA (J. Am. Vet. Med. Assoc.).* 203:300–306.

6. Pober, J.S., and R.S. Cotran. 1990. Overview: the role of endothelial cells in inflammation. *Transplantation.* 50:537–541.

7. Vane, J.R., E.E. Anggard, and R.M. Botting. 1990. Regulatory functions of the vascular endothelium. *N. Engl. J. Med.* 323:27–36.

8. Gimbrone, M.A., Jr., E.J. Shefton, and S.A. Cruise. 1978. Isolation and primary culture of endothelial cells from human umbilical vessels. *Tiss. Cult. Assoc. Man.* 4:813–818.

9. Zünd, G., S. Uezono, G.L. Stahl, A.L. Dzus, F.X. McGowan, P.R. Hickey, and S.P. Colgan. 1997. Hypoxia enhances endotoxin-stimulated induction of functional intercellular adhesion molecule-1 (ICAM-1). *Am. J. Physiol. (Cell. Physiol.).* 273:C1571–C1580.

10. Zünd, G., D.P. Nelson, E.J. Neufeld, A.L. Dzus, J. Bischoff, J.E. Mayer, and S.P. Colgan. 1996. Hypoxia enhances stimulus-dependent induction of E-selectin on aortic endothelial cells. *Proc. Natl. Acad. Sci. USA.* 93:7075–7080.

11. Dharmsathaphorn, K., and J.L. Madara. 1990. Established intestinal cell lines as model systems for electrolyte transport studies. *Methods Enzymol.* 192: 354–389.

12. Parkos, C.A., C. Delp, M.A. Arnaout, and J.L. Madara. 1991. Neutrophil migration across a cultured intestinal epithelium. Dependence on a CD11b/CD18-mediated event and enhanced efficiency in the physiologic direction. *J. Clin. Invest.* 88:1605–1612.

13. Zünd, G., J.L. Madara, A.L. Dzus, C.S. Awtrey, and S.P. Colgan. 1996. Interleukin 4 and interleukin 13 differentially regulate epithelial chloride secretion. *J. Biol. Chem.* 271:7460–7464.

14. Smith, J.J., and M.J. Welsh. 1993. Fluid and electrolyte transport by cultured human airway epithelia. *J. Clin. Invest.* 91:1590–1597.

15. Madara, J.L., T.W. Patapoff, B. Gillece-Castro, S.P. Colgan, C.A. Parkos, C. Delp, and R.J. Mrsny. 1993. 5′-adenosine monophosphate is the neutrophil-derived paracrine factor that elicits chloride secretion from T84 intestinal epithelial cell monolayers. *J. Clin. Invest.* 91:2320–2325.

16. Serhan, C.N. 1989. On the relationship between leukotriene and lipoxin production by human neutrophils: evidence for differential metabolism of 15(S)-HETE and 5-HETE. *Biochim. Biophys. Acta.* 1004:158–168.

17. Taylor, C.T., S.J. Lisco, C.S. Awtrey, and S.P. Colgan. 1998. Hypoxia inhibits cyclic nucleotide-stimulated epithelial ion transport: role for nucleotide cyclases as oxygen sensors. *J. Pharmacol. Exp. Ther.* 284:568–575.

18. McCormick, B.A., C.A. Parkos, S.P. Colgan, D.K. Carnes, and J.L. Madara. 1998. Apical secretion of a pathogen-elicited epithelial chemoattractant activity in response to surface colonization of intestinal epithelia by *Salmonella typhimurium. J. Immunol.* 160:455–466.

19. Grynkiewicz, G., M. Poenie, and R.Y. Tsien. 1985. A new generation of Ca^{2+} indicators with greatly improved fluorescent properties. *J. Biol. Chem.* 260:3440–3450.

20. Hofman, P., L. D'Andrea, D. Carnes, S.P. Colgan, and J.L. Madara. 1996. Intestinal epithelial cytoskeleton selectively constrains lumen-to-tissue migration of neutrophils. *Am. J. Physiol.* 271:C312–C320.

21. McCormick, B.A., S.P. Colgan, C. Delp-Archer, S.I. Miller, and J.L. Madara. 1993. *Salmonella typhimurium* attachment to human intestinal epithe-

lial monolayers. Transcellular signaling to subepithelial neutrophils. *J. Cell Biol.* 123:895–907.

22. Colgan, S.P., M.B. Resnick, C.A. Parkos, C. Delp-Archer, A.E. Bacarra, P.F. Weller, and J.L. Madara. 1994. Interleukin-4 directly modulates function of a model human intestinal epithelium. *J. Immunol.* 153:2122–2129.

23. Taylor, C.T., A.L. Dzus, and S.P. Colgan. 1998. Autocrine regulation of intestinal epithelial permeability induced by hypoxia: role for basolateral release of tumor necrosis factor-α (TNF-α). *Gastroenterology.* 114:657–668.

24. Colgan, S.P., V.M. Morales, J.L. Madara, S.P. Balk, and R.S. Blumberg. 1996. IFN-γ modulates CD1d expression on intestinal epithelia. *Am. J. Physiol.* 271:C276–C283.

25. Kawakami, M., S. Ishibashi, H. Ogawa, T. Murase, F. Takaku, and S. Shibata. 1986. Cachectin/TNF as well as interleukin-1 induces prostacyclin synthesis in cultured vascular endothelial cells. *Biochem. Biophys. Res. Comm.* 141:482–485.

26. Maier, J.A.M., T. Hla, and T. Maciag. 1990. Cyclooxygenase is an immediate-early gene induced by interleukin-1 in human endothelial cells. *J. Biol. Chem.* 265:10805–10808.

27. Shen, T.Y., and C.A. Winter. 1977. Chemical and biological studies on indomethacin, sulidac, and their analogs. *Adv. Drug Res.* 12:90–245.

28. Futaki, N., S. Takahashi, M. Yokoyama, I. Arai, S. Higuchi, and S. Otomo. 1994. NS-398, a new anti-inflammatory agent, selectively inhibits prostaglandin G/H synthase/cyclooxygenase (COX-2) activity in vitro. *Prostaglandins.* 47:55–59.

29. Madara, J.L., C.A. Parkos, S.P. Colgan, R.J. MacLeod, S. Nash, J. Matthews, C. Delp, and W.S. Lencer. 1992. Cl^- secretion in a model intestinal epithelium induced by a neutrophil-derived secretagogue. *J. Clin. Invest.* 89:1938–1944.

30. Strohmeier, G.R., S.M. Reppert, W.I. Lencer, and J.L. Madara. 1995. The A2b adenosine receptor mediates cAMP responses to adenosine receptor agonists in human intestinal epithelia. *J. Biol. Chem.* 270:2387–2394.

31. Falardeau, P., J.A. Oates, and A.R. Brash. 1981. Quantitative analysis of two dinor urinary metabolites of prostaglandin I_2. *Anal. Biochem.* 115:359–367.

32. Brash, A.R., E.K. Jackson, C.A. Saggese, J.A. Lawson, J.A. Oates, and G.A. Fitzgerald. 1983. Metabolic disposition of prostacyclin in humans. *J. Pharmacol. Exp. Ther.* 226:78–87.

33. Whittaker, N., S. Bunting, J. Salmon, S. Moncada, J.R. Vane, R.A. Johnson, D.R. Morton, J.H. Kinner, R.R. Gorman, J.C. McGuire, and F.F. Sun. 1976. The chemical structure of prostaglandin X (prostacyclin). *Prostaglandins.* 12:915–928.

34. Rosenkranz, B., C. Fischer, I. Reimann, K.E. Weimer, G. Beck, and J.C. Frolich. 1980. Identification of the major metabolite of prostacyclin and 6-keto-prostaglandin $F_{1\alpha}$ in man. *Biochim. Biophys. Acta.* 619:207–213.

35. Barrett, K.E. 1993. Positive and negative regulation of chloride secretion in T84 cells. *Am. J. Physiol.* 265:C859–C868.

36. Breyer, M.D., H.R. Jacobson, and R.M. Breyer. 1996. Functional and molecular aspects of real prostaglandin receptors. *J. Am. Soc. Nephrol.* 7:8–17.

37. Waxman, K. 1996. Shock: ischemia, reperfusion and inflammation. *New Horizons.* 4:153–160.

38. Cook, B.H., E.R. Wilson, and A.E. Taylor. 1971. Intestinal fluid loss in hemorrhagic shock. *Am. J. Physiol.* 221:1494–1498.

39. Maier, R.V., and E.M. Bulger. 1996. Endothelial changes after shock and injury. *New Horizons.* 4:211–223.

40. Haglund, U.H., L. Hulten, C. Ahren, and O. Lungren. 1975. Mucosal lesions in the human intestine in shock. *Gut.* 16:979–984.

41. Blikslager, A.T., M.C. Roberts, J.M. Rhoades, and R.A. Argenzio. 1997. Prostaglandins I2 and E2 have a synergistic role in rescuing epithelial barrier function in porcine ileum. *J. Clin. Invest.* 100:1928–1933.

42. Hinterleitner, T.A., J.I. Saada, H.M. Berschneider, D.W. Powell, and J.D. Valentich. 1996. IL-1 stimulates intestinal myofibroblast COX gene expression and augments activation of Cl^- secretion in T84 cells. *Am. J. Physiol. (Cell. Physiol).* 271:C1262–C1266.

43. Berschneider, H.M., and D.W. Powell. 1992. Fibroblasts modulate intestinal secretory responses to inflammatory mediators. *J. Clin. Invest.* 89:484–489.

44. Michiels, C., T. Arnould, I. Knott, M. Dieu, and J. Remacle. 1993. Stimulation of prostaglandin synthesis by human endothelial cells exposed to hypoxia. *Am. J. Physiol.* 264:C866–C874.

45. Nawroth, P.P., D.M. Stern, K.L. Kaplan, and H.L. Nossel. 1984. Prostacyclin production by perturbed bovine aortic endothelial cells in culture. *Blood.* 64:801–806.

46. Vane, J.R., and R.M. Botting. 1995. Pharmacologic profile of prostacyclin. *Am. J. Cardiol.* 75:3A–10A.

47. Lellouche, F., A. Fradin, G. Fitzgerald, and J. Maclouf. 1990. Enzyme immunoassay measurement of the urinary metabolites of thromboxane A_2 and prostacyclin. *Prostaglandins.* 40:297–310.

48. Namba, T., H. Oida, Y. Sugimoto, A. Kakizuka, M. Negishi, A. Ichikawa, and S. Narumiya. 1994. cDNA cloning of a mouse prostacyclin receptor: multiple signaling pathways and expression in thymic medulla. *J. Biol. Chem.* 269:9986–9992.

49. Katsuyama, M., Y. Sugimoto, T. Namba, A. Irie, M. Negishi, S. Narumiya, and A. Ichikawa. 1994. Cloning and expression of a cDNA for the human prostacyclin receptor. *FEBS Lett.* 344:74–78.

50. Hebert, R.L., L. Regnier, and L.N. Peterson. 1995. Rabbit cortical collecting ducts express a novel prostacyclin receptor. *Am. J. Physiol. (Renal Fluid Electrolyte Physiol.).* 268:F145–F154.